ACS APPLIED MATERIALS & INTERFACES

Research Article

www.acsami.org

Constructing Covalent Interface in Rubber/Clay Nanocomposite by Combining Structural Modification and Interlamellar Silylation of Montmorillonite

Chao Zha,[†] Wencai Wang,[‡] Yonglai Lu,*[,‡] and Liqun Zhang*[,†,‡]

[†]Key Laboratory of Beijing City on Preparation and Processing of Novel Polymer Materials, Beijing University of Chemical Technology, Beijing 100029, China

[‡]State Key Laboratory of Organic–Inorganic Composites, Beijing University of Chemical Technology, Beijing 100029, China

Supporting Information

ABSTRACT: Strong interfacial interaction and nanodispersion are necessary for polymer nanocomposites with expectations on mechanical performance. In this work, montmorillonite (MMT) was first structurally modified by acid treatment to produce more silanol groups on the layer surface. This was followed by chemical modification of γ-methacryloxy propyl trimethoxysilane molecule (KH570) through covalent grafting with the silanol groups. ^{29}Si and ^{27}Al magic angle spinning (MAS) NMR results revealed the microstructural changes of MMT after acid treatment and confirmed the increase of silanol groups on acid-treated MMT surfaces. Thermogravimetric analysis indicated an increase in the grafted amount of organosilane on the MMT surface. X-ray diffraction (XRD) showed that the functionalization process changed the highly ordered stacking structure of the MMT mineral into a highly disordered structure, indicating successful grafting of organosilane to the interlayer surface of the crystalline sheets. The styrene–butadiene rubber (SBR)/MMT nanocomposites were further prepared by co-coagulating with SBR latex and grafted-MMT aqueous suspension. During vulcanization, a covalent interface between modified MMT and rubber was established through peroxide-radical-initiated reactions, and layer aggregation was effectively prevented. The SBR/MMT nanocomposites had highly and uniformly dispersed MMT layers, and the covalent interfacial interaction was finally achieved and exhibited high performance.

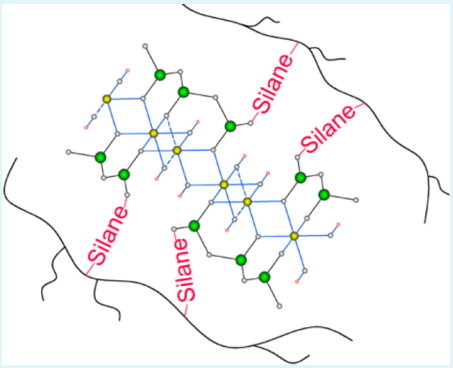

KEYWORDS: *montmorillonite, acid treatment, silane, rubber, latex compounding method*

1. INTRODUCTION

Since the Toyota research group[1] reported a nylon-6/montmorillonite nanocomposite over two decades ago, polymer/clay nanocomposites have attracted much attention from both academic and industrial fields.[2] When dispersed into a rubber matrix, clay minerals can remarkably improve the mechanical properties and provide the composites with some novel performance, such as impressive gas barrier properties.[3−5] It was reported that the properties of the nanocomposites were strongly dependent on both the dispersion of clay layers and the interfacial interaction between the clay and rubber matrix.[6,7] Only when clay platelets are completely exfoliated within the rubber matrix and the interfacial interaction is optimized, will the potential of performance of the nanocomposite be fully realized.[7−9]

In order to achieve high dispersion of clay in rubber matrix, various methods have been developed, such as melt method, solution method, in situ polymerization method, latex method, and so on. Among these methods, latex compounding method[10−12] using water as a medium is an eco-friendly and promising means to prepare rubber/clay nanocomposites. Some clay minerals, like montmorillonite, have excellent swelling properties in water and could be delaminated into single nanolayers to form a stable aqueous suspension;[11,12] also, the medium of rubber latex is water in which the rubber latex particles are uniformly dispersed. So, a stable aqueous mixture of clay and rubber latex particles could be easily obtained in which the clay nanolayers and rubber particles are stably and uniformly dispersed. Rubber/clay nanocomposites could be prepared by co-coagulating the mixture of clay and rubber latex, and there is no need for further mechanical mixing because the good dispersion of clay in water could be kept in the rubber matrix after the flocculation. An advantage for latex compounding method is in situ organic modification for clay in water medium can be conducted before co-coagulating rubber latex and clay aqueous suspension.[6,13] Such an organic modification is very important for nanocompounding to achieve a good co-coagulating effect and to construct a better interfacial interaction.

Received: July 7, 2014
Accepted: October 17, 2014
Published: October 17, 2014

Montmorillonite (MMT) is the most commonly used clay mineral for preparing rubber/clay nanocomposites. It is a member of the family of 2:1 layered silicates and consists of two-dimensional layers where an edge-shared alumina octahedral sheet is sandwiched between two silica tetrahedral sheets.[2] The thickness of MMT layers is about 1 nm. Isomorphic substitution within the layers generates negative charges that are counterbalanced by metal ions situated inside the galleries.[2,4] Obviously, in this pristine state, the inorganic MMT is immiscible with hydrophobic rubber, such as styrene−butadiene rubber (SBR), and the poor physical interaction leads to poor mechanical properties of the composites. In order to make clay layers more miscible with the polymer, one must convert the hydrophilic clay surface to an organophilic one. The traditional methodologies generally utilized organic quaternary ammonium salt to directly modify inorganic clay by exchanging with the metal ions present inside the galleries.[2,14] This modification of clay by organic alkylammonium salts can increase the interlayer distance of the clay mineral and greatly improve the compatibility between rubber and clay layers. But the interaction between organic clay and rubber is still weak due to the nature of the van der Walls force and the improvement of performance of nanocomposite with a noncovalent interface is limited.[6,15]

Silane coupling agent, as an effective interfacial modifier in rubber industry, can greatly enhance the interface through the formation of covalent bonds between the rubber and inorganic filler. Recently, the grafting reaction between silane molecules and clay layers was widely reported.[16−19] The covalent bonding between clay and organosilane is formed through condensation reactions between silane and the surface silanol groups.[20,21] However, plate-like clay surfaces such as montmorillonite have reactive hydroxyl groups only at the edges of individual layers and at relatively low contents.[17,20,22,23] As a result, only limited organosilane can be linked at the edges,[22−24] and the external functionalized edge area of grafted-MMT is small as compared to the interlayer surface, which will lead to limited improvement in interfacial interaction between MMT and polymer matrix.[25] Therefore, grafting more organic functions in the interlayer region of MMT is critical. It has been reported that acid treatment could result in the formation of more hydroxyl groups on the clay surface and increase the grafted amount of organosilane on clay surface.[22,26,27] Unfortunately, the mechanism of acid treatment is still undefined, and the silylated acid-treated MMT has never been used to fill rubber to improve the interfacial interaction.

In this work, acid treatment was employed to destruct the MMT structure to introduce more active sites on the surface of nanolayers and improve the reactivity of the MMT surface with coupling agents. The γ-methacryloxy propyl trimethoxysilane (KH570) was then utilized as an effective interfacial modifier for MMT and its SBR nanocomposites. The microstructure and surface property of the acid-treated MMT and functionalized MMT were studied using various techniques. Further, the latex compounding was employed to prepare functionalized SBR/MMT nanocomposites, that is, a mixture of functionalized-MMT aqueous suspension and SBR latex was co-coagulated by adding flocculation agent. The interfacial covalent interaction was finally and completely realized via peroxide vulcanization, in which the peroxide radicals chemically linked double bonds of KH570 and SBR macromolecules. The resultant nanocomposites demonstrated much higher modulus and tensile strength. To the best of our knowledge, similar research has not been reported.

2. EXPERIMENTAL SECTION

2.1. Materials. Sodium montmorillonite powder was purchased from Siping Liufangzi Aska Bentonite Co., Ltd., China, with a cationic exchange capacity (CEC) of 78 mequiv/100 g. SBR latex with a styrene content of 23 wt % was purchased from Jilin petrochemical Co., Ltd., China. The organosilane used in this work was γ-methacryloxy propyl trimethoxysilane (KH570), which was purchased from Nanjing Shuguang Chemical Co., China. The peroxide curing agent dicumyl peroxide (DCP) was industrial-grade and used as received.

2.2. Preparation of Acid-Treated MMT. MMT aqueous suspension with a solid content of 2.0 wt % was prepared according to procedure in our previous work.[28] A certain amount of concentrated HCl was added to make up different concentrations. The suspension was magnetically stirred at 60 °C for 3 h. After acid treatment, the solid phase was separated from supernatant liquid by centrifugation at 5000 rpm for 1 h. The MMT was washed intensively with deionized water. The pH of the supernatant after it was washed was in the range of 6−7. Then, the sample was dried in a vacuum oven at 60 °C for 24 h. The as-prepared MMT sample was crushed to smaller units by using a mortar. In the following discussion, the acid-treated MMT powders are coded as nHMMT, and *n* indicates the concentration of hydrochloric acid (*n* mol/L).

2.3. Preparation of γ-Methacryloxy Propyl Trimethoxysilane-Modified HMMT. The preparation of acid-treated MMT aqueous suspension with a solid content of 2.0 wt % was the same as that of the pristine MMT aqueous suspension. The required amount of KH570, corresponding to 3 mequiv of coupling agent per gram of MMT, was added into the MMT aqueous suspension and stirred for 5 h at 80 °C. The suspension was centrifuged at 5000 rpm for 1 h to separate solid phase of KH570/MMT hybrids. To remove the excess silane, we washed the solid phase by being dispersing it in ethanol under vigorous stirring at 65 °C for 1 h, which was followed by centrifugation. The procedure was repeated three times. The resultant product was dried at 60 °C under vacuum for 24 h and then ground to powder for characterization. To confirm that the unreacted coupling agents were completely removed, we washed the final powders with toluene by Soxhlet extraction for 24 h because the Soxhlet extraction is considered to be an effective means to remove unreacted and adsorbed coupling agents.[29] The TGA analysis of modified MMT before and after Soxhlet extraction could be found in Figure S1 (Supporting Information). The silane-grafted HMMT samples were coded as nHMMT-*g*-KH570.

The functionalized HMMT before drying procedure was dispersed in the deionized water to form aqueous suspension with a solid content of 2.0 wt %.

2.4. Preparation of SBR/MMT Nanocomposites. The ratio of MMT to SBR in composite was kept at 10 g/100 g. The SBR/MMT nanocomposites were prepared by latex compounding method, and the procedure cab be found in our previous work.[6] The SBR/MMT coagulated compounds were obtained by co-coagulating the mixture of modified MMT and SBR latex in 1% hydrochloric acid solution. The coagulated compounds and 0.5 phr DCP were mixed on a two-roll mill for 10 min. Then, the compounds were vulcanized at 160 °C for the optimum cure time (T90).

2.5. Characterizations. XRD analyses were carried out on a D/Max 2500 VB2+/PC X-ray diffractometer (Rigaku, Japan) with Cu/Kα1 radiation, and two patterns were employed: pattern I (accelerating voltage, electric current, and scanning speed were 40 kV, 50 mA, and 0.5°/min, respectively) and pattern II (accelerating voltage, electric current, and scanning speed were 40 kV, 2000 mA and 10°/min, respectively). FTIR spectra were recorded using a TENSOR27 spectrometer (Bruker, Germany) and KBr pressed-disk technique (1 mg of sample and 200 mg KBr) were used. The morphologies of modified MMT samples were recorded by a Hitachi S-4800 scanning electron microscope (SEM). The specific surface area

of MMT powders was determined by combining the Nitrogen adsorption measurements in Quantachrome Autosorb-1-MP automated gas adsorption system and the Brunauer–Emmett–Teller (BET) method. Dynamic light scattering performed in Zetasizer Nano ZS (Malvern, UK) was used to determine the particle size of MMT in aqueous suspension.

The ^{29}Si and ^{27}A1 magic angle spinning (MAS) NMR spectra of acid-treated MMT in powder form were recorded on a Bruker AV300 spectrometer at 59.63 and 78.62 MHz, respectively, using TMS and the solution of $AlCl_3$ as the external references. The sample spinning frequency was 5 and 8 kHz, respectively. To avoid saturation, we selected a 15 s recycle delay between successive accumulations for each ^{29}Si spectrum.

Thermogravimetric analysis was performed on a STARe system TGA (Mettler-Toledo, Switzerland). The amount of grafted silane was calculated by eq 1 according to the report.[18]

$$\text{Grafted amount (mequiv/g)} = \frac{10^3 W_{200-600}}{(100 - W_{200-600})M} \quad (1)$$

where M (g/mol) is the molecular weight of the grafted silane molecules (M = 206 for KH570) and $W_{200-600}$ is the weight loss between 200 and 600 °C corresponding to degradation of silane.[18]

Dynamical mechanical rheology analysis was performed with the rheometer RPA 2000 (Alpha Technologies, Akron, Ohio) at 60 °C with the frequency of 1 Hz. High-resolution transmission electron microscopies (HR-TEM) were conducted on a JEM 3010 high-resolution transmission electron microscope (JEOL, Japan) and the ultrathin section samples were used.

The tensile properties tests were conducted on an Instron-type tensile testing machine at 23 °C according to ASTM D412 (Method A). Shore A hardness of the nanocomposite was measured according to ASTM D2240, using an XY-1 type A durometer (No. 4 Chemical Machinery Plant of Shanghai Chemical Equipment Co. Ltd., China).

3. RESULTS AND DISCUSSION

3.1. Acidification of Montmorillonite. Montmorillonite is a naturally occurring 2:1 layered silicate. The crystal structure is shown in Chart1. Isomorphic substitution within the layers,

Chart 1. Illustration of Crystalline Structure of Montmorillonite

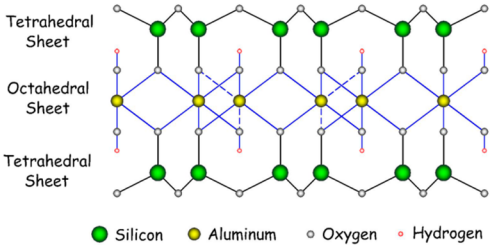

including some Al substitution by Fe and Mg in the octahedral sheet and little Si substitution by Al in the tetrahedral sheet, generates negative charges that are counterbalanced by the interlayer cations.[2,30] The surface hydroxyl groups are very few and mostly located at the edges of individual layers. Montmorillonite also contains intralayer Al–OH groups, but these groups are buried inside atomic planes of the layered structure and believed to hardly react with organosilane molecules.[31,32]

It was widely reported that acid activation of montmorillonite follows this process:[30,33,34] (1) protons penetrate into the layers and interlamellar cations are replaced; (2) protons attack the OH groups, starting with those close to the isomorphic substitution and the layers partially dissolved by leaching out Al^{3+}, Fe^{3+}, and Mg^{2+} from the silicate; and (3) the Al–O octahedral sheets dissolved entirely by leaching out Al^{3+}, generating hydrous amorphous silica from the tetrahedral sheet.

The XRD patterns of the pristine and acid-treated MMT are presented in Figure 1. The d_{100} at 20° was used as an internal

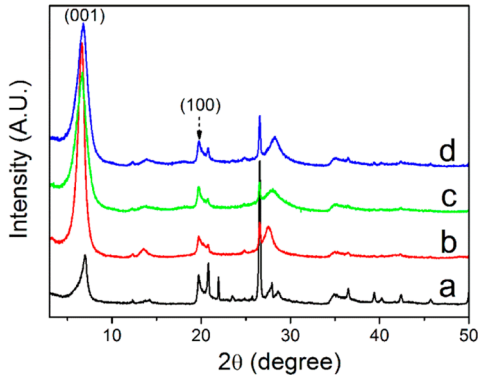

Figure 1. X-ray diffraction patterns (pattern II) of (a) pristine MMT, (b) 0.02HMMT, (c) 0.1HMMT, and (d) 0.5HMMT.

standard to standardize diffractograms in relation to the percentage of MMT crysatlline.[35] The intensity of the characteristic 001 peak for each acid-treated MMT powder increased distinctly, which may be due to the dissolution of most amorphous mineral particles and reflects an increase in the regularity of the crystallite. A broaden peak at a 2θ value of 28° corresponding to silica is observed in the acid-treated MMT, indicating the generation of amorphous silica.[36] The increase in the intensity at (001) diffraction peak of acid-treated MMT has never been reported because the acid concentration we applied was much lower than that reported previously.[37] With the concentration of hydrochloric acid increasing, the acid treatment leads to some alteration of the crystal structure of the minerals which is seen from lowering and broadening of the (001) peaks on the patterns, indicating a decrease in the regularity of the mineral structure and little dissolution of structural ions. The XRD patterns show that the crystal structure of MMT was mostly preserved and not affected significantly, even by the activation with the maximum HCl concentration of 0.5 mol/L. However, there was a slight increase from 1.24 to 1.30 nm in the interlayer spacing of acid-treated MMT compared to pristine MMT, indicating the generation of interlayer hydroxyl groups.

Infrared spectroscopy was used to study the microstructure of pristine MMT and acid-treated MMT. Figure 2 illustrates infrared spectra of the samples. In the spectrum of pristine MMT, a band appeared near 3630 cm^{-1}, corresponding to the stretching vibrations of structural Al–OH and Mg–OH which are intralayer hydroxyl groups and can not be reactive with silane.[32] Meanwhile, IR spectra of these samples show a broad band centered near 3440 cm^{-1} and a clear band at 1640 cm^{-1}, which are attributed to the interlayer water in the MMT. The spectra of acid-treated MMT show a gradual shift of the Si–O band from 1042 to 1050 cm^{-1}, indicating the generation of amorphous silica.[27] The slight shift strongly supports that the chemical structure of MMT after acid treatment was remained unchanged.

^{29}Si and ^{27}Al NMR spectroscopies further illustrate the effect of acid on the microstructure of MMT. The ^{29}Si and ^{27}Al MAS NMR spectra of pristine and acid-treated MMT are shown in

dx.doi.org/10.1021/am504426j | ACS Appl. Mater. Interfaces 2014, 6, 18769–18779

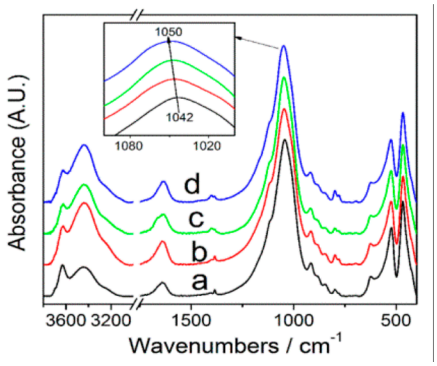

Figure 2. Infrared spectra of (a) pristine MMT, (b) 0.02HMMT, (c) 0.1HMMT, and (d) 0.5HMMT.

Figure 3. The $Q^3(0Al)$ at −92.2 ppm attributed to SiO_4 groups in the tetrahedral sheet was used as an internal standard to

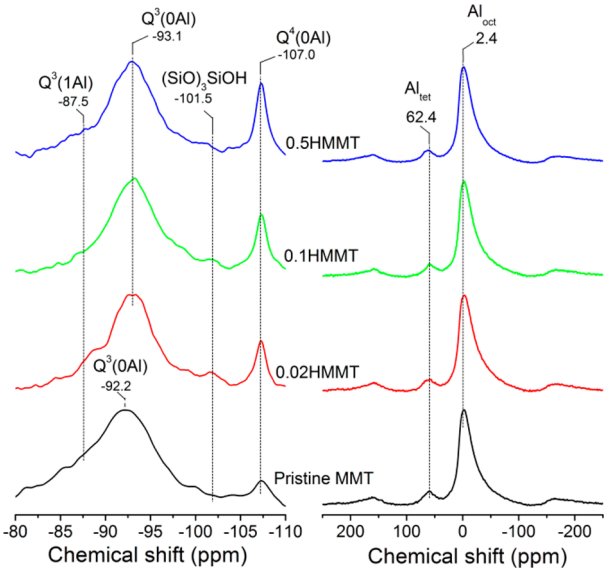

Figure 3. (Left) ^{29}Si MAS NMR spectra and (right) ^{27}Al MAS NMR spectra of the pristine and acid-treated MMT powders.

standardize strength in relation to the percentage of clay in ^{29}Si MAS NMR spectra. So, the strength of other signals was a relative one. $Q^3(1Al)$ at −87.5 ppm is attributed to one tetrahedron in which Al for Si substitution occurs in the tetrahedral sheet. The signal of Q^4 at −107 ppm demonstrates the presence of quartz, which is an impurity in pristine MMT. There is no signal of Q^2 in the ^{29}Si MAS NMR spectrum of pristine MMT, attributed to isolated silanol groups present at the silicate sheet edges.[17] After acidification, an additional signal at −101 ppm for Si−OH was recorded in the ^{29}Si MAS NMR spectra of acid-treated MMT, which was not found in pristine MMT. This demonstrates the successful enrichment of hydroxyl groups at the edges and faces of layered silicate after acid treatment at an appropriate acid concentration. With the concentration of hydrochloric acid increasing, the signal at −107 ppm corresponding to amorphous silica became stronger, as a result of the dissolution of Al ions in the octahedral sites and formation of amorphous silica.[30]

Tkac et al.[30] suggested that the rates of dissolution of tetrahedral and octahedral Al (Al_{tet} and Al_{oct}) within layers in acid solution are comparable and Si atoms bearing OH groups are formed in the first stage of dissolution of the clay. In our experiment, the leaching out of Al_{tet} was confirmed by the weakening of the signal corresponding to $Q^3(1Al)$ at −87.5 ppm and the chemical shift changing of $Q^3(0Al)$ from −92.2 to −93.1 ppm after acid treatment. Figure 3 (right) shows that the proportions of Al_{tet} and Al_{oct} in MMT remain unchanged after acid treatment, which confirms that the dissolution of tetrahedral and octahedral Al occurs at the same rate. As discussed above, the acid treatment procedure can be summarized in Chart2. This model has the similar concept of

Chart 2. Schematic Process of the Acid Treatment

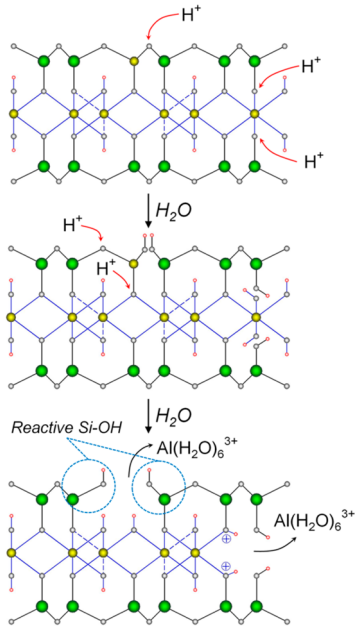

"patched detetrahedration" for montmorillonite in dissolution alkaline media proposed by Takahashi et al.[38] Dissolution of one tetrahedral Al (Al_{tet}) generates three Si−OH groups and one Al−OH group. These Si−OH groups are believed to be exposed on the surface of layered structure, which can react with coupling agent molecules, while the hydroxyl groups generated by dissolution of octahedral Al are still buried inside atomic planes of the layered structure and hardly react with the coupling agent molecules. We are not sure about how many Si−OH groups among the hydroxyls generated by acid treatment are exposed on the surface of layered structure, so the quantitative analysis of reactive Si−OH groups is hard to carry out by NMR analysis.

The result that enrichment of Si−OH by acidification confirmed by ^{29}Si MAS NMR is consistent with that reported in the literature,[39] whereas the result that higher concentration of acid led to fewer hydroxyl groups is reported for the first time. In a higher concentration of acid solution, amorphous silica formed through the condensation reactions of Si−OH groups,[30] which may be responsible for fewer hydroxyl groups. Therefore, controlling the dissolution degree of MMT is crucial to maximize the hydroxyl number.

Nitrogen BET surface areas were measured for the pristine and acid-treated samples. A slight increase in surface area was observed with the increase of the concentration of hydrochloric acid (Table 1), which suggests that the surface cracks and voids formed due to the removal of amorphous components that may plug some pores on the surface and between layers.[34]

Table 1. Interlayer Spacing and Specific Surface Area of Pristine and Acid-Treated MMT

samples	d_{001} (nm)[a]	S_{spec} (m^2/g)[b]
pristine MMT	1.24	21.3
0.02HMMT	1.30	22.8
0.1HMMT	1.30	28.4
0.5HMMT	1.30	33.9

[a]Determined by XRD. [b]External surface area.

3.2. Functionalization of MMT. The FTIR spectra of pristine MMT and silane grafted MMT are shown in Figure 4.

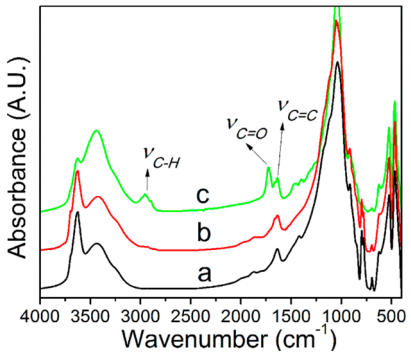

Figure 4. Infrared spectra of (a) pristine MMT, (b) MMT-*g*-KH570, and (c) 0.02HMMT-*g*-KH570.

Figure 4c shows the characteristic vibrations of the C═O group ($\nu_{C=O}$, 1729 cm^{-1}) and the CH_2 and CH_3 groups (ν_{CH}, 2870, 2920, and 2980 cm^{-1}; and δ_{CH}, 1380 cm^{-1}) of the KH570 molecule. The stretching vibration of the C═C bond at 1637 cm^{-1} overlaps with the δ_{OH} deformation band at 1636 cm^{-1} of physically absorbed H_2O. These results indicate that acid reaction favors the enrichment of active hydroxyl groups on the surface of MMT platelets, which is favorable to organosilane grafting process.

Before the quantitative analysis of the amount of grafted silane, the grafted MMT samples were extensively washed to remove the unreacted organosilane. Figure 5 shows the TGA curves of pristine MMT and KH570-grafted MMT. Table 2 shows the weight loss between 200 and 600 °C and the grafted amount of these samples, and Table S1 in Supporting Information shows the detailed information on TGA data. Acid-treated MMT with more reactive Si−OH have more organosilane coverage. The grafted amount of 0.02HMMT

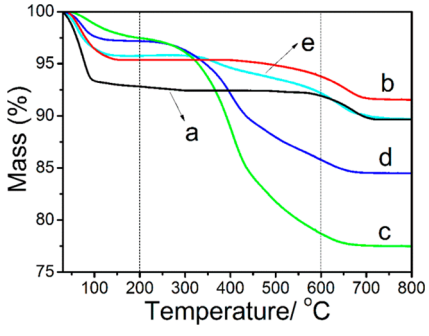

Figure 5. TGA degradation profiles of (a) pristine MMT, (b) MMT-*g*-KH570, (c) 0.02HMMT-*g*-KH570, (d) 0.1HMMT-*g*-KH570, and (e) 0.5HMMT-*g*-KH570.

Table 2. Interlayer Spacing, Specific Surface Area, and Grafted Amount of Pristine and Functionalized MMT

samples	$W_{200-600}$ (%)[a]	grafted amount (mmol/g)[b]	d_{001} (nm)[c]	S_{spec} (m^2/g)[d]
pristine MMT	0.8		1.24	21.3
MMT-*g*-KH570	1.6	0.1	1.24	35.6
0.02HMMT-*g*-KH570	18.8	1.1		182.3
0.1HMMT-*g*-KH570	11.4	0.6	1.30	100.2
0.5HMMT-*g*-KH570	3.6	0.2	1.30	52.7

[a]Weight loss between 200 and 600 °C. [b]Determined using eq 1. [c]Determined by XRD. [d]External surface area.

sample reached 1.1 mmol/g, while pristine MMT only had 0.1 mmol/g. The grafted amount decreased with the increase of the HCl concentration, which is in agreement with the relative amount of Si−OH group determined by NMR spectroscopies. However, some of the Si−OH groups determined by NMR spectroscopy are still buried inside atomic planes of the layered structure and hardly react with the organosilane molecules, which means the grafted amount is not quantitatively consistent with the result of NMR. And we cannot ignore the fact that the oligomerization of KH570 occurred in a water medium and that the oligomer could covalently attach to the MMT surface in the grafting reaction,[40] which may lead to the grafted amount being much higher than the content of active hydroxyl groups on MMT surface (Chart3a).

Chart 3. Schematic Representation of the Functionalized HMMT[a]

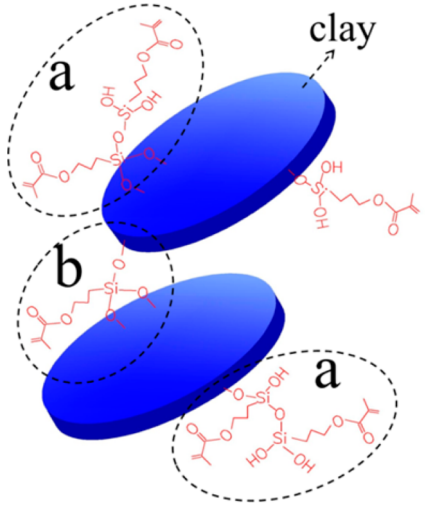

[a]Structure a shows the silane oligomer covalently attaching to MMT surface. Structure b shows KH570 molecule linking two individual MMT platelets to form an attached clay stack.

The XRD patterns of the functionalized MMT powders are shown in Figure 6. The (001) peak broadening and weakening of the hybrids compared to both pristine and acid-treated MMT suggests that grafting modification induces a stacking disorder in the clay particles. The (001) diffraction of the hybrids with high organic content was weaker, which cannot be found even in the 0.02HMMT-*g*-KH570 sample, indicating that the highly ordered stacking structure of the MMT mineral became a highly disordered structure. These results imply that the KH570 molecule successfully graft to the interlayer surface of the MMT crystalline sheets, which was realized before only

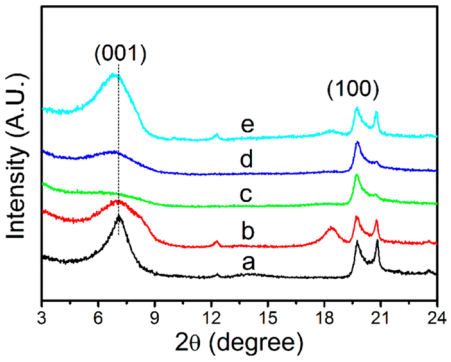

Figure 6. X-ray diffraction patterns (pattern II) of (a) pristine MMT, (b) MMT-*g*-KH570, (c) 0.02HMMT-*g*-KH570, (d) 0.1HMMT-*g*-KH570, and (e) 0.5HMMT-*g*-KH570.

by conventional ion exchange method using aminosilane.[19] An increase in interlayer spacing of the interlamellar grafted MMT was not found. It may be due to the nature of KH570, which could not self-assemble to orderly arrange between two clay layers to form ordered intercalation structure.

The BET surface areas of the grafted HMMT samples are also shown in Table 2. There is a significant increase in surface area for grafted MMT compared to that of the pristine and acid-treated MMT. The higher grafted amount leads to higher surface area which was also observed by Shanmugharaj et al.[41] It is noted that the BET surface area determined for montmorillonite represents interactions with only the outer particle surfaces because the interlayer of clay is inaccessible to nitrogen molecules.[20] The significantly increase from 21.3 to 182.3 m^2/g indicates the internal surfaces were partly exposed caused by silane grafting at the interlayer surface of MMT and the disordered layer structure. It was reported that the specific surface areas substantially decreased with the grafting agent occupying the micropores,[42] which is because the organosilane was covalently linked only at the edge −OH groups of MMT platelets. Only when the clay layers with reactive hydroxyl groups in the interlayer region are exfoliated in the reaction medium, could interlamellar grafting be realized. Therefore, using water as the dispersing medium is critical to realize interlamellar grafting.

Figure 7 shows the surface morphology of silane-grafted MMT. The 0.02HMMT-*g*-KH570 with the highest grafted amount has a rough surface (Figure 7d). However, the pristine MMT and the MMT-*g*-KH570 with lower grafted amount show smooth surfaces. This result also demonstrated that the grafting reaction took place to form silane oligomer coverage on the layers.

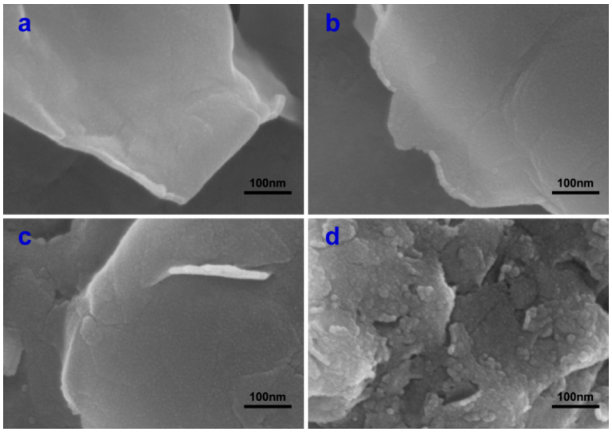

Figure 7. SEM morphology of (a) pristine MMT, (b) MMT-*g*-KH570, (c) 0.02HMMT, and (d) 0.02HMMT-*g*-KH570.

3.3. Aqueous Suspensions of Modified MMT. The dispersion of MMT in polymer nanocomposite prepared by latex compounding method strongly depends on the state of MMT aqueous suspension. Therefore, in this work, the stability of the modified MMT aqueous suspension and the particle size of modified MMT in water were characterized. The 0.02HMMT-*g*-KH570 with the highest organic content was chosen because the centration of acid caused the least effect on the crystal structure of MMT.

Figure 8 shows the digital photos of MMT aqueous suspension both before and after the same centrifugation process. Because MMT has good swelling property in water and the surface is normally hydrophilic, a stable aqueous suspension was obtained. After centrifugation, only a part of inorganic MMT happened to subside (Figure 8b,d). The KH570-grafted MMT suspension (Figure 8c) exhibit the same result as the inorganic MMT suspension, indicating that the hydrophilic surface is not significantly changed due to the fact that the organic grafting only occurred at the edges of clay platelets. The grafted HMMT with the highest organic content (Figure 8e) was precipitated completely after centrifugation. The success of interlamellar grafting (Chart S1, Supporting Information) and the high silane content increase the hydrophobicity of the modified clay, which is detrimental to the dispersion of the modified MMT in water.

The average diameter of the modified sample in suspension was determined by dynamic light scattering (DLS; Table 3). Comparing the particle size of grafted MMT with that of inorganic MMT, a slight increase is found. The KH570 modifier with three Si−OH groups can react with more than one hydroxyl group on the MMT surface, which offers the possibility to form covalent bridges between MMT layers and generate irreversibly attached clay stacks (Chart3b). However, this slight increase of particle size indicates that the grafted MMT still could be satisfactorily dispersed in water.

3.4. MMT/SBR Nanocomposites. *3.4.1. MMT Dispersion in Nanocomposites.* The 0.02HMMT-*g*-KH570 with the highest organic content was chosen to fill in the SBR matrix. In the following, XRD and HR-TEM experiments were carried out in order to investigate the dispersion of MMT in nanocomposites.

The XRD spectra of SBR/MMT vulcanizates recorded by pattern I are shown in Figure 9. The SBR/MMT vulcanizate and MMT-*g*-KH570/SBR vulcanizate show distinct diffraction peaks at about $2\theta = 6.4°$, corresponding to the stacked structures. However, the 0.02HMMT-*g*-KH570/SBR vulcanizate is nearly amorphous to X-rays, demonstrating a highly dispersed state of MMT in the SBR matrix. A tiny peak corresponding to interlayer spacing of about 4.70 nm emerges in the pattern of 0.02HMMT-*g*-KH570/SBR vulcanizate, indicating the intercalation of rubber molecules.[6]

Basically, the MMT dispersion in coagulated compounds depends on the state in the aqueous suspension. The DLS result has proved the three clay samples have similar dispersion state in aqueous suspension. Therefore, it is reasonable to conclude that the dispersion of clay in the three coagulated compounds is similar and that the big difference in the clay dispersion within the three vulcanizates results from the

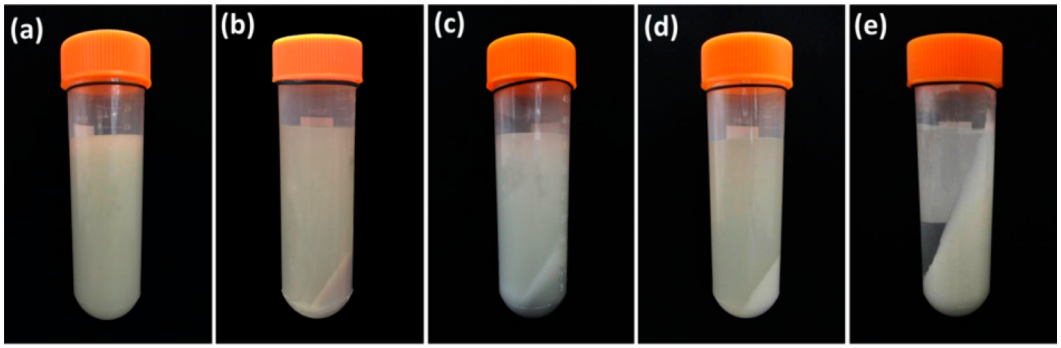

Figure 8. Stability of 2 wt % MMT aqueous suspension. Pristine MMT aqueous suspension (a) before and (b) after centrifugation. (c) MMT-*g*-KH570 aqueous suspension after centrifugation. (d) 0.02HMMT aqueous suspension after centrifugation. (e) 0.02HMMT-*g*-KH570 aqueous suspension after centrifugation. Centrifugation was conducted at 5000 rpm for 20 min.

Table 3. Particle Size of the Acid-Treated MMT and Functionalized MMT

samples	Z-average (nm)
pristine MMT	507
MMT-*g*-KH570	516
0.02HMMT	489
0.02HMMT-*g*-KH570	564

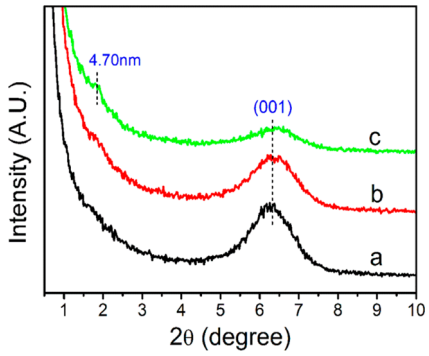

Figure 9. XRD patterns (pattern I) of SBR/MMT(10) vulcanizates. (a) SBR/MMT nanocomposite, (b) SBR/MMT-*g*-KH570 nanocomposite, and (c) SBR/0.02HMMT-*g*-KH570 nanocomposite.

different degrees of clay aggregation. In our previous works, we proved that intensive shearing during processing and high temperature and pressure during vulcanization would cause the distinct aggregation of clay platelets in rubber matrix.[43] The high-resolution TEM images are shown in Figure 10. Without KH570 grafting, most MMT layers aggregated into big agglomerates with diameter of about 50−300 nm. For the SBR/MMT-*g*-KH570 nanocomposite, the dispersion of MMT is slightly improved and the agglomerate size becomes much smaller, indicating that a small amount of KH570 grafting on the edge could improve the dispersion of MMT effectively. When the grafted amount reaches 1.1 mmol/g, the grafting reaction significantly improves the clay dispersion, and most of the layers are highly and uniformly dispersed in vulcanizates as thin layers with thickness down to 5−15 nm. In Figure 10c,c′, the dispersion of grafted MMT in the SBR/0.02HMMT-*g*-KH570 vulcanizate is better than that in coagulated compound. That is because the intensive shearing during processing makes highly silylated MMT aggregates break into smaller units, while for the unmodified SBR/MMT nanocomposites, the intensive shearing is detrimental to the dispersion of the inorganic MMT in rubber matrix, as proven in our previous work.[43] After curing, the covalent interface between clay and rubber is established, and the excellent dispersion of grafted clay in the unvulcanized compound is kept in the vulcanizate.

Digital photos of SBR/MMT nanocomposite sheets are shown in Figure 11. The three coagulated compound sheets had high and similar transparency, which indicates that the dispersion of MMT in the nanocomposites is excellent. The transparency of the three vulcanizate sheets was much different. The SBR/0.02HMMT-*g*-KH570 vulcanizate had the highest transparency, indicating the best dispersion of clay. The result is consistent with those observed by the above XRD and HR-TEM results. On the one hand, the high content of KH570 grafted on clay surface improves compatibility between MMT and rubber macromolecules, which benefits the dispersion of MMT further. On the other hand, KH570 molecules undergo grafting onto macromolecular chains during vulcanization, which effectively prevented the aggregation of clay caused by high temperature and pressure. These effects directly improve the dispersion of MMT in the SBR matrix. Chart4 schematically illustrates the interlamellar silylation of acid-treated MMT and the process of construction of covalent interface between acid-treated MMT and rubber.

3.4.2. Curing Behavior and Dynamic Properties of Nanocomposites. Table 4 shows the curing behavior of SBR/MMT nanocomposites. Compared to the SBR/MMT nanocomposite, the curing time of the grafted SBR/MMT nanocomposites was obviously shortened, indicating that organosilane could accelerate the curing process. With the grafted amount increasing, the maximum torque obviously increased, and the minimum torque was basically unchanged. The basically same minimum torque reflects the same dispersion of clay in three unvulcanized compounds. The increase in maximum torque is attributed to improved dispersion of clay and excellent interaction between clay and rubber in organically modified SBR/MMT vulcanizates, which is consistent with the results observed in the above XRD and HR-TEM results.

The dynamic properties of the SBR/MMT vulcanizates were characterized by dynamic strain sweeps. Figure 12-1 shows the strain amplitude dependence of storage modulus (G') of the SBR/MMT nanocomposites. The SBR/0.02HMMT-*g*-KH570 nanocomposite (Figure 12c) exhibited the highest modulus at the strain amplitude, indicating the formation of the strongest filler network. There are two factors determining the increase of storage modulus: (1) the good dispersion of MMT in the grafted SBR/MMT nanocomposite increases the interfacial area

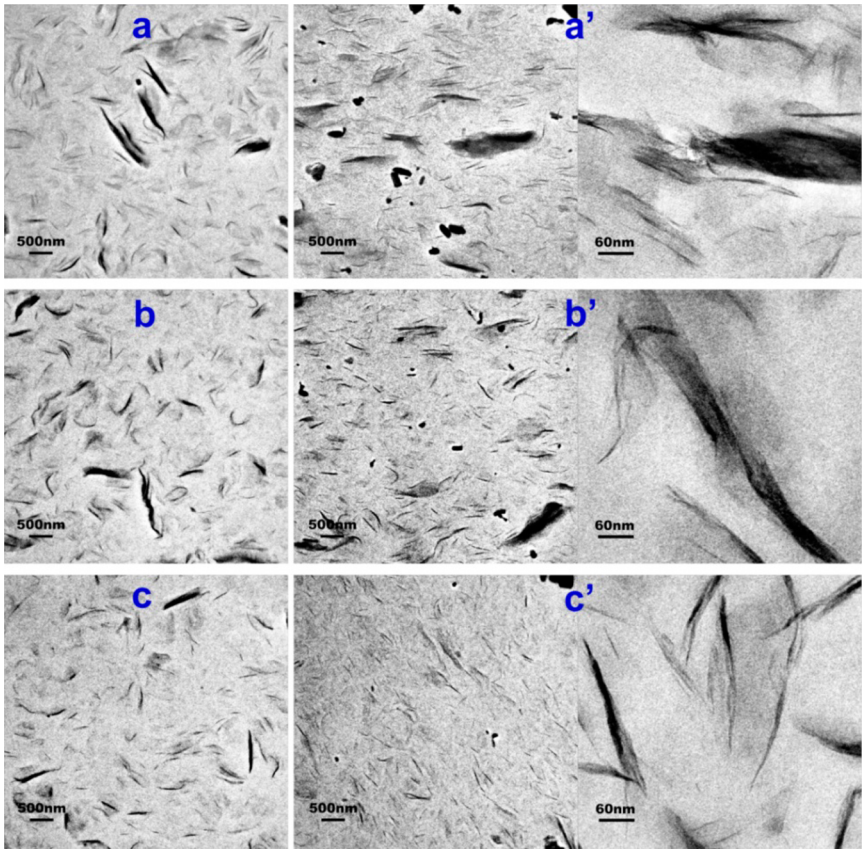

Figure 10. HR-TEM images of SBR/MMT(10) nanocomposites. SBR/MMT (a) coagulated compound and (a′) vulcanizate. SBR/MMT-*g*-KH570 (b) coagulated compound and (b′) vulcanizate. SBR/0.02HMMT-*g*-KH570 (c) coagulated compound and (c′) vulcanizate.

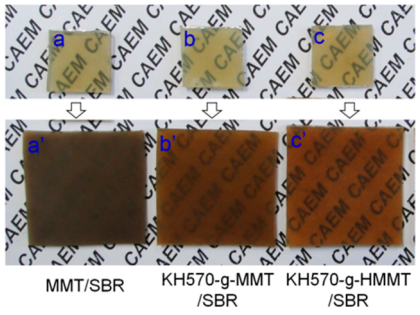

Figure 11. Digital photos of SBR/MMT(10) nanocomposite sheets (1 mm). SBR/MMT (a) coagulated compound and (a′) vulcanizate. SBR/MMT-*g*-KH570 (b) coagulated compound and (b′) vulcanizate. SBR/0.02HMMT-*g*-KH570 (c) coagulated compound and (c′) vulcanizate.

between MMT and rubber, and (2) a covalent interface between clay and rubber matrix was established through KH570 molecules and the MMT-rubber interaction was remarkably improved. Figure 12-2 shows the strain amplitude dependence of loss factor for nanocomposites. It is revealed that the loss factor of nanocomposites is decreased with increasing the grafted amount of silane, indicating the reduction in mobility of rubber chains.[7] The distinct decrease in loss factor of SBR/0.02HMMT-*g*-KH570 nanocomposite strongly confirmed the significantly enhanced interfacial interaction.

3.4.3. Static Mechanical Properties of SBR/MMT Nanocomposites. Table 5 shows the static mechanical properties of SBR/MMT nanocomposites. All the mechanical properties are significantly enhanced by introducing the silane coupling agent. The stress at certain strain and hardness are increased significantly. The tensile strength and stress at 300% strain of SBR/MMT nanocomposite are 7.9 and 2.4 MPa, respectively.

Chart 4. Silylation of Acid-Treated MMT and Preparation of Rubber/MMT Nanocomposite by Latex Compounding Method

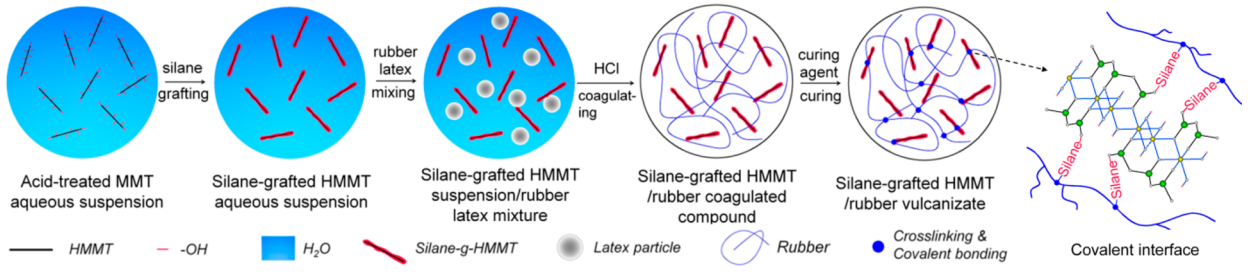

dx.doi.org/10.1021/am504426j | ACS Appl. Mater. Interfaces 2014, 6, 18769−18779

Table 4. Curing Characteristic of SBR/MMT Nanocomposites

samples	scorch time (min)	cure time (min)	minimum torque, ML (Nm)	maximum torque, MH (Nm)	MH−ML (Nm)
SBR/MMT	0.88	10.00	8.11	17.03	8.92
SBR/MMT-*g*-KH570	0.83	6.53	7.72	18.41	10.69
SBR/MMT-*g*-KH570	0.75	5.58	7.35	23.14	15.79

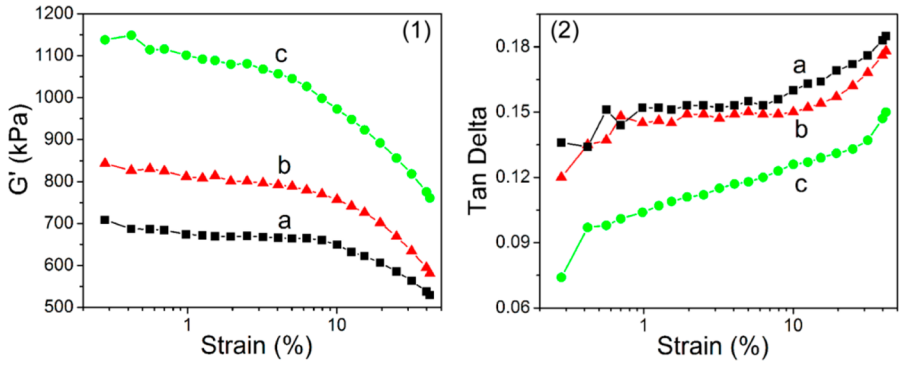

Figure 12. Strain amplitude dependence of (1) storage modulus (G') and (2) loss factor of (a) SBR/MMT vulcanizate, (b) SBR/MMT-*g*-KH570 vulcanizate, and (c) SBR/0.02HMMT-*g*-KH570 vulcanizate.

Table 5. Mechanical Properties of the MMT(10)/SBR Nanocomposites

nanocomposite	tensile strength (MPa)	elongation at break (%)	stress at 100% strain (MPa)	stress at 300% strain (MPa)	Shore A hardness	permanent set (%)
SBR/MMT	7.9	835	1.1	2.4	49	28
SBR/MMT-*g*-KH570	7.6	737	1.1	2.9	52	28
SBR/MMT-*g*-KH570	11.5	451	2.0	7.6	59	16

For SBR/0.02HMMT-*g*-KH570 nanocomposite, the two properties are improved to 11.5 and 7.6 MPa, respectively.

Figure 13 represents the stress−strain curves of nanocomposites and different stress−strain behaviors were found.

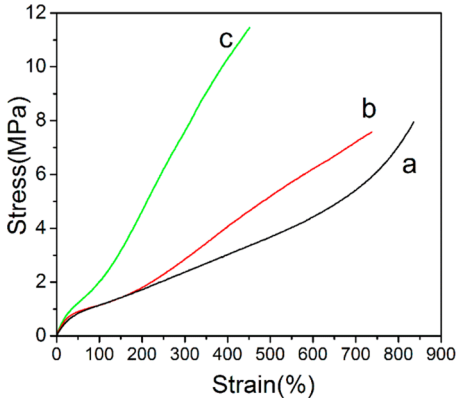

Figure 13. Stress−strain curves of (a) SBR/MMT vulcanizate, (b) SBR/MMT-*g*-KH570 vulcanizate, and (c) SBR/0.02HMMT-*g*-KH570 vulcanizate.

For SBR/MMT nanocomposite, the stress increases slowly at the initial range of strain from 0 to 650%, and after that, the stress has a rapid increase when the strain is more than 650%. In this situation, van der Waals is the main interaction between clay and macromolecules so that polymer chains on the surface of clay could slip under the external force. During large deformation, the rubber chains physically absorbing onto clay surface are forced to slide along the MMT surface giving rise to tensile orientation of rubber chains leading to a dramatic increase of stress. All of these are advantageous to improve the tensile strength, but not to achieve a high modulus and high rigidity. For the SBR/MMT-*g*-KH570 nanocomposite, two kinds of interaction exist between clay and rubber: (1) van der Waals bonding as the main interaction between clay and macromolecules; (2) covalent bonding between clay edges and rubber. So, the mechanical properties of SBR/MMT-*g*-KH570 nanocomposite are better than those of SBR/MMT nanocomposites. But the interaction between MMT-*g*-KH570 and macromolecular chains is not strong enough because of the low grafted amount of silane, so the improvement on the mechanical properties is limited. The higher content of KH570 grafting on both the edge and interlayer region of acid-treated clay built a much stronger covalent boding between rubber and clay and the interfacial interaction is significantly enhanced. That is why the SBR/0.02HMMT-*g*-KH570 nanocomposite possesses excellent tensile strength and the highest stress at 300% strain.

The different clay−rubber interaction result in the different stress−strain behaviors of nanocomposites. The grafting reactions establish the strong covalent interface between rubber and acid-treated MMT through KH570 linkages, which are responsible for the remarkably enhanced properties. Additionally, the significantly improved dispersion of MMT also benefits the improvement of mechanical properties.

4. CONCLUSIONS

In this work, surface modification of MMT by acid treatment and silane grafting were successfully demonstrated. The active hydroxyl groups on the surface of MMT have been increased by acid-treatment at an appropriate acid concentration. By using the acid-treated MMT, the organosilane was covalently linked at the edges and on the interlamellar surface of MMT, and the grafted amount of organosilane was significantly increased. The

realization of interlamellar grafting changed the highly ordered stacking structure of the pristine clay mineral into a highly disordered structure, and the formation of silane oligomer coverage on the layers make the hydrophilic silicate surface become an organophilic one.

Latex compounding method was used to prepare the SBR/MMT nanocomposites. With the formation of a chemical bridge between MMT and rubber during the curing, the dispersion of MMT in rubber matrix was evidently improved, and the interfacial interaction was remarkably enhanced. Finally, the SBR/MMT nanocomposites had highly and uniformly dispersed MMT layers, and covalent interfacial interaction was finally achieved and exhibited high performance.

■ ASSOCIATED CONTENT

Supporting Information

TGA degradation profiles of grafted MMT powders before and after Soxhlet extraction, detailed TGA data of the pure SBR and grafted MMT powders, and the schematic of grafting reaction. This material is available free of charge via the Internet at http://pubs.acs.org.

■ AUTHOR INFORMATION

Corresponding Authors

*E-mail: luyonglai@mail.buct.edu.cn. Tel: +86-10- 64456158. Fax: +86-10-64433964.

*E-mail: zhanglq@mail.buct.edu.cn. Tel: +86-10-64434860. Fax: +86-10-64433964.

Notes

The authors declare no competing financial interest.

■ ACKNOWLEDGMENTS

The authors appreciate the financial support from the National Natural Science Foundation of China under Grant Nos. 51221002, 51320105012 and 51373010 and the National Basic Research Program of China (973 Program) under Grant No. 2011CB932603.

■ REFERENCES

(1) Usuki, A.; Kojima, Y.; Kawasumi, M.; Okada, A.; Fukushima, Y.; Kurauchi, T.; Kamigaito, O. Synthesis of Nylon 6-Clay Hybrid. *J. Mater. Res.* **1993**, *8*, 1179−1184.

(2) Pavlidou, S.; Papaspyrides, C. D. A Review on Polymer-Layered Silicate Nanocomposites. *Prog. Polym. Sci.* **2008**, *33*, 1119−1198.

(3) Gatos, K. G.; Karger-Kocsis, J. Effect of the Aspect Ratio of Silicate Platelets on the Mechanical and Barrier Properties of Hydrogenated Acrylonitrile Butadiene Rubber (HNBR)/Layered Silicate Nanocomposites. *Eur. Polym. J.* **2007**, *43*, 1097−1104.

(4) Suprakas, S. R.; Masami, O. Polymer/Layered Silicate Nanocomposites: A Review from Preparation to Processing. *Prog. Polym. Sci.* **2003**, *28*, 1539−1641.

(5) Lu, Y. L.; Li, Z.; Yu, Z. Z.; Tian, M.; Zhang, L. Q.; Mai, Y. W. Microstructure and Properties of Highly Filled Rubber/Clay Nanocomposites Prepared by Melt Blending. *Compos. Sci. Technol.* **2007**, *67*, 2903−2913.

(6) Jia, Q. X.; Wu, Y. P.; Wang, Y. Q.; Lu, M.; Zhang, L. Q. Enhanced Interfacial Interaction of Rubber/Clay Nanocomposites by a Novel Two-Step Method. *Compos. Sci. Technol.* **2008**, *68*, 1050−1056.

(7) Chen, W. W.; Wu, S.; Lei, Y. D.; Liao, Z. F.; Guo, B. C.; Liang, X.; Jia, D. M. Interfacial Structure and Performance of Rubber/Boehmite Nanocomposites Modified by Methacrylic Acid. *Polymer* **2011**, *52*, 4387−4395.

(8) Wang, Z. H.; Liu, J.; Wu, S. Z.; Wang, W. C.; Zhang, L. Q. Novel Percolation Phenomena and Mechanism of Strengthening Elastomers by Nanofillers. *Phys. Chem. Chem. Phys.* **2010**, *12*, 3014−3030.

(9) Fröhlich, J.; Niedermeier, W.; Luginsland, H. D. The Effect of Filler−Filler and Filler−Elastomer Interaction on Rubber Reinforcement. *Composites, Part A* **2005**, *36*, 449−460.

(10) Wang, Y. Q.; Zhang, H. F.; Wu, Y. P.; Yang, J.; Zhang, L. Q. Preparation, Structure, and Properties of a Novel Rectorite/Styrene−Butadiene Copolymer Nanocomposite. *J. Appl. Polym. Sci.* **2005**, *96*, 324−328.

(11) Wu, Y. P.; Wang, Y. Q.; Zhang, H. F.; Wang, Y. Z.; Yu, D. S.; Zhang, L. Q.; Yang, J. Rubber−Pristine Clay Nanocomposites Prepared by Co-Coagulating Rubber Latex and Clay Aqueous Suspension. *Compos. Sci. Technol.* **2005**, *65*, 1195−1202.

(12) Varghese, S.; Karger-Kocsis, J. Natural Rubber-Based Nanocomposites by Latex Compounding with Layered Silicates. *Polymer* **2003**, *44*, 4921−4927.

(13) Jia, Q. X.; Wu, Y. P.; Xu, Y. L.; Mao, H. H.; Zhang, L. Q. Combining in Situ Organic Modification of Montmorillonite and the Latex Compounding Method to Prepare High-Performance Rubber-Montmorillonite Nanocomposites. *Macromol. Mater. Eng.* **2006**, *291*, 218−226.

(14) Fischer, H. Polymer Nanocomposites: From Fundamental Research to Specific Applications. *Mater. Sci. Eng., C* **2003**, *23*, 763−772.

(15) Huskić, M.; Žigon, M.; Ivanković, M. Comparison of the Properties of Clay Polymer Nanocomposites Prepared by Montmorillonite Modified by Silane and by Quaternary Ammonium Salts. *Appl. Clay Sci.* **2013**, *85*, 109−115.

(16) Park, M.; Shim, I. K.; Jung, E. Y.; Choy, J. H. Modification of External Surface of Laponite by Silane Grafting. *J. Phys. Chem. Solids* **2004**, *65*, 499−501.

(17) He, H. P.; Duchet, J.; Galy, J.; Gerard, J. F. Grafting of Swelling Clay Materials with 3-Aminopropyltriethoxysilane. *J. Colloid Interface Sci.* **2005**, *288*, 171−176.

(18) Herrera, N. N.; Letoffe, J. M.; Putaux, J. L.; David, L.; Elodie, B. L. Aqueous Dispersions of Silane-Functionalized Laponite Clay Platelets. A First Step toward the Elaboration of Water-Based Polymer/Clay Nanocomposites. *Langmuir* **2004**, *20*, 1564−1571.

(19) Piscitelli, F.; Posocco, P.; Toth, R.; Fermeglia, M.; Pricl, S.; Mensitieri, G.; Lavorgna, M. Sodium Montmorillonite Silylation: Unexpected Effect of the Aminosilane Chain Length. *J. Colloid Interface Sci.* **2010**, *351*, 108−115.

(20) Song, K.; Sandí, G. Characterization of Montmorillonite Surfaces after Modification by Organosilane. *Clays Clay Miner.* **2001**, *49*, 119−125.

(21) Shen, W.; He, H. P.; Zhu, J. X.; Yuan, P.; Frost, R. L. Grafting of Montmorillonite with Different Functional Silanes via Two Different Reaction Systems. *J. Colloid Interface Sci.* **2007**, *313*, 268−273.

(22) Rausell-Colom, J. A.; Serratosa, J. M. In *Chemistry of Clays and Clay Minerals*; Newman, A. C. D., Ed.; Wiley-Interscience: New York, 1987; pp 371−422.

(23) Bourlinos, A. B.; Jiang, D. D.; Giannelis, E. P. Clay−Organosiloxane Hybrids: A Route to Cross-Linked Clay Particles and Clay Monoliths. *Chem. Mater.* **2004**, *16*, 2404−2410.

(24) Yu, D.; Lin, Z.; Li, Y. Octadecenylsuccinic Anhydride Pickering Emulsion Stabilized by γ-Methacryloxy Propyl Trimethoxysilane Grafted Montmorillonite. *Colloids Surf., A* **2013**, *422*, 100−109.

(25) Manna, A. K.; Tripathy, D. K.; De, P. P.; De, S. K.; Chatterjee, M. K.; Peiffer, D. G. Bonding between Epoxidized Natural Rubber and Clay in Presence of Silane Coupling Agent. *J. Appl. Polym. Sci.* **1999**, *72*, 1895−1903.

(26) Paul, B.; Martens, W. N.; Frost, R. L. Organosilane Grafted Acid-Activated Beidellite Clay for the Removal of Non-Ionic Alachlor and Anionic Imazaquin. *Appl. Surf. Sci.* **2011**, *257*, 5552−5558.

(27) Madejová, J.; Pálková, H.; Pentrák, M.; Komadel, P. Near-Infrared Spectroscopic Analysis of Acid-Treated Organo-Clays. *Clays Clay Miner.* **2009**, *57*, 392−403.

(28) Lu, M.; Wang, Y.; Wu, Y.; Quan, Y.; Wu, X.; Zhang, L.; Guo, B. Preparing Exfoliated MMT/Polymer Nanocomposites by Combined Latex Compounding and Spray-Drying. *Macromol. Mater. Eng.* **2012**, *297*, 20−25.
(29) Zhang, Y.; Gittins, D. I.; Skuse, D.; Cosgrove, T.; Van, D. J. S. Nonaqueous Suspensions of Surface-Modified Kaolin. *Langmuir* **2007**, *23*, 3424−3431.
(30) Tkac, I.; Komadel, P.; Mueller, D. Acid-Treated Montmorillonites: A Study by ^{29}Si and ^{27}Al MAS NMR. *Clay Miner.* **1994**, *29*, 11−19.
(31) Carrado, K. A.; Komadel, P. Acid Activation of Bentonites and Polymer-Clay Nanocomposites. *Elements* **2009**, *5*, 111−116.
(32) Morris, H. D.; Bank, S.; Ellis, P. D. Aluminum-27 NMR Spectroscopy of Iron-Bearing Montmorillonite Clays. *J. Phys. Chem.* **1990**, *94*, 3121−3129.
(33) Breen, C.; Madejová, J.; Komadel, P. Correlation of Catalytic Activity with Infrared, ^{29}Si MAS NMR and Acidity Data for HCl-Treated Fine Fractions of Montmorillonites. *Appl. Clay Sci.* **1995**, *10*, 219−230.
(34) Jozefaciuk, G.; Bowanko, G. Effect of Acid and Alkali Treatments on Surface Areas and Adsorption Energies of Selected Minerals. *Clays Clay Miner.* **2002**, *50*, 771−783.
(35) Dean, K.; Yu, L.; Wu, D. Y. Preparation and Characterization of Melt-Extruded Thermoplastic Starch/Clay Nanocomposites. *Compos. Sci. Technol.* **2007**, *67*, 413−421.
(36) Kumar, P.; Jasra, R. V.; Bhat, T. S. G. Evolution of Porosity and Surface Acidity in Montmorillonite Clay on Acid Activation. *Ind. Eng. Chem.* **1995**, *34*, 1440−1448.
(37) Madejová, J.; Pálková, H.; Jankovič, Ľ. Degradation of Surfactant-Modified Montmorillonites in HCl. *Mater. Chem. Phys.* **2012**, *134*, 768−776.
(38) Takahashi, T.; Ohkubo, T.; Suzuki, K.; Ikeda, Y. High Resolution Solid-State NMR Studies on Dissolution and Alteration of Na-Montmorillonite under Highly Alkaline Conditions. *Microporous Mesoporous Mater.* **2007**, *106*, 284−297.
(39) He, H. P.; Guo, J. G.; Xie, X. D.; Lin, H. F.; Li, L. Y. A Microstructural Study of Acid-Activated Montmorillonite from Choushan, China. *Clay Miner.* **2002**, *37*, 337−344.
(40) Herrera, N. N.; Letoffe, J. M.; Reymond, J. P.; Bourgeat-Lami, E. Silylation of Laponite Clay Particles with Monofunctional and Trifunctional Vinyl Alkoxysilanes. *J. Mater. Chem.* **2005**, *15*, 863−871.
(41) Shanmugharaj, A. M.; Rhee, K. Y.; Ryu, S. H. Influence of Dispersing Medium on Grafting of Aminopropyltriethoxysilane in Swelling Clay Materials. *J. Colloid Interface Sci.* **2006**, *298*, 854−859.
(42) Tonle, I. K.; Ngameni, E.; Njopwouo, D.; Carteret, C.; Walcarius, A. Functionalization of Natural Smectite-Type Clays by Grafting with Organosilanes: Physico-Chemical Characterization and Application to Mercury(II) Uptake. *Phys. Chem. Chem. Phys.* **2003**, *5*, 4951−4961.
(43) Quan, Y. N.; Wang, Y. Q.; Wu, Y. P.; Lu, M.; Zha, C.; Wu, X. H.; Zhang, L. Q. Network Transformations of Highly Dispersed MMT/SBR Nanocomposites During Processing. *J. Appl. Polym. Sci.* **2013**, *130*, 113−119.